Vol: 4 -- Issue: 1, 2025
WORLDWIDE JOURNAL OF PHYSICS
Http://wwjop.com/index.php/Journal
Editor@wwjop.com
ISSN: 3006-0486 (Print)
ISSN: 3006-0486 (Online)

DEVELOPMENT OF ADVANCED TURBULENCE MODELS FOR BETTER PREDICTION OF TURBULENT FLOWS

Saima Kousar[1*], Hafiz Muhammad Ali[2]
[1]COMSATS University Islamabad, Lahore Campus
[2]Government College University (GCU), Lahore
*Corresponding Author E-Mail: saimakhan@yahoo.com

Abstract

Turbulence remains one of the most challenging phenomena in fluid mechanics, characterized by chaotic, multiscale, and three dimensional fluctuations in velocity, pressure, and vorticity. Accurate prediction of turbulent flows is crucial across engineering applications, from aerospace and automotive design to energy systems and environmental modeling. Conventional turbulence modeling approaches, such as Reynolds Averaged Navier–Stokes (RANS) and Large Eddy Simulation (LES), have made significant contributions to computational fluid dynamics (CFD), but limitations persist in capturing complex flow separation, anisotropy, and transitional regimes. This study focuses on the development of advanced turbulence models that integrate higher order closure schemes, non local pressure–strain formulations, and hybrid RANS–LES frameworks. The proposed models aim to enhance predictive accuracy in high Reynolds number flows while maintaining computational efficiency. Numerical experiments are conducted on canonical test cases—including turbulent boundary layers, backward facing step flows, and bluff body wakes—to evaluate model performance against experimental data and Direct Numerical Simulation (DNS) benchmarks. Results demonstrate notable improvements in the prediction of mean velocity profiles, turbulence intensities, and separation/reattachment points compared to baseline models. The findings highlight the potential of these advanced turbulence models to bridge the gap between computational feasibility and physical accuracy, providing a robust framework for the next generation of CFD tools in industrial and scientific applications.

Article History

Received:
January 25, 2025

Revised:
February 06, 2025

Accepted:
March 15, 2025

Available Online:
June 30, 2025

Keywords: “Turbulence Modeling”, “Computational Fluid Dynamics”, “Reynolds Averaged Navier–Stokes”, “Large Eddy Simulation”, “Hybrid Rans–Les”, “Advanced Closure Models”.

INTRODUCTION

Turbulence is probably one of the most difficult and unresolved issues in classical physics. It occurs when the particles of the fluid experience a chaotic and random movement on a broad scale of the time and space (Davidson, et al., 2015). It is also fundamental in far-ranging technical and natural systems such as the drag of aerodynamic surfaces, the dispersion of pollution gasses in the atmosphere, the transmission of energy through ocean currents, and much more (Pope, et al., 2000). Nonlinearity of the NavierStokes equations and the large number of categories of possible eddies that can influence each other, make it extremely difficult to calculate the significant characteristics of turbulent flows computation fluid dynamics (CFD). Even though Direct Numerical Simulation (DNS) provides the most accurate model of turbulence since all the scales of the motion have been resolved, it cannot be applied to most of the practical flows within high Reynolds numbers (Moin, et al., 1998).

In order to manage this issue, turbulence models have been designed so as to make estimations of how the unresolved scales impact the resolved flow field. The cost of making prediction is reduced in Reynolds-Averaged Nav. Stokes (RANS) models and other traditional models because the governing equations are simplified through statistical averaging that makes the prediction process easier and affordable (Wilcox, et al., 2006). The most common RANS model, which is also the kkk-e\epsilonϵ-model and kkk-o\omegaomega model, has found good use in engineering applications because it is resilient and effective (Launder, et al., 1974). These models, however, usually struggle to well represent such complex aspects of the flow as large separation, anisotropic turbulence and transitional behaviour.

Another significant method of defining turbulence is through massive Eddy Simulation (LES). During this procedure, the large eddies which contain much energy are solved directly with the smaller ones being modelled by the subgrid-scale (SGS) models (Sagaut, et al., 2006). LES has greater accurateness than RANS particularly in strong and unstable flow structures. Nonetheless, this value remains difficult to calculate, particularly in high Reynolds number wall-bounded flows (Piomelli, et al., 2015). A compromise solution between cost and accuracy in finding a compromise would be Detached Eddy Simulation (DES) and Scale-Adaptive Simulation (SAS), which employs RANS modelling near the walls and LES modelling in regions that have remained separated or unsteady (Spalart, et al., 1997).

Turbulence modelling continues to pose a lot of issues to be resolved despite such advancements. RANS models are insensitive to nonlocal such as the pressure Strain redistribution, and hurriedly beset by isotropy neglectful predictions of turbulence. LES methods need high spatial resolution close to walls and SGS models need to be handled with sensitivity to prevent convergence problems (Pope, et al., 2000). Both approaches may also be incompetent with the changing flows with laminar, turbulent and separated region simultaneously. The constraints drive the invention of new turbulence models which may be more predictive of the physics of the complex flows, as well as computationally feasible in industrial CFD.

As of late, researchers have controlled to enlarge higher-order closure arrangements that make a beeline on the Reynolds stress anisotropy and nonlocal transportation impact (Craft et al., 1996). Nonlinear eddy viscosity models (NLEVMs) are attained by adding higher-order factors of strain and rotation rate to the classical linear formulation of eddy viscosity. This will facilitate the prediction of swirling and rotating flows (Speziale, et al., 1991). Higher fidelity is afforded again by Reynolds Stress Models (RSMs), and even by high-fidelity turbulence IM, which solve transport equations governing the Reynolds stress itself, and thus directly simulate both anisotropy and pressure-strain of the turbulence spectrum (Launder, et al., 1975). These models are computationally more expensive to execute upon a computer and may suffer numerical instability.

The other possible approach is closing the gap between machine learning and high-fidelity DNS/LES data in informing and ameliorating closure models through data-driven turbulence modelling (Duraisamy, et al., 2019). Such type of techniques attempt to overcome model deficiencies in a systematic manner, adapt to the different flow regimes and also increase the level of forecast performance across a broad-spectrum of application. PINNs have found success at imposing the constraint of modelling turbulence on learning algorithms to be some form of what is being intended to be consistent with the laws of physics (Raissi, et al., 2019).

Since more accurate predictions are required in multi-physics problems like responding flows in combustion systems, multiphase flows in energy production, and environmental flows with buoyancy effects, the need of having more improved turbulence models is also increasing (Veynante et al., 2002). When such occurs, turbulence combines with the processes of chemical reactions, phase change as well as stratification thus becoming increasingly difficult to model.In this research, we focus on advancing turbulence modeling by developing higher-fidelity closure schemes that integrate nonlinear eddy viscosity formulations, nonlocal pressure–strain models, and hybrid RANS–LES frameworks. The proposed approach aims to provide a better balance between accuracy and computational cost, validated against canonical turbulent flows such as channel flows, backward-facing step flows, and bluff-body wakes. By benchmarking against both experimental data and DNS results, we aim to assess the performance improvements over conventional models and provide insights into the pathways for developing the next generation of turbulence modeling tools.

METHODOLOGY

The developed and tested improved turbulence models were generated and tested in a mixed-methods experimental approach to be able to make turbulent flow simulations more accurate. Rebekka used both a qualitative description and calculation. The research was aimed at discovering what is wrong in the existing models and propose superior models as per actual and computerized tests. Our approach was a hybrid approach that integrated direct numerical simulation (DNS), large eddy simulation (LES), and Reynolds- averaged Navier-Stokes (RANS) to examine turbulence structures in the flows of various regimes with various levels of detail.

Canonical turbulent flows which we used as ground truth to calibrate the model were channel flows and turbulent jet examined through high-resolution DNS in the first step. These DNS datasets were generated using a spectral method-based solution whereby spatial discretisation was refined to the Kolmogorov scale. During the 2nd phase, RANS visions such as k-e models, k-omega SST, and Spalart-Allmaras models, among others were employed and their boundaries determined by comparison with the DNS benchmark data. To begin with, the SmagorinskyLilly subgrid-scale model was applied so as to capture energy-containing eddies. After that, more intricate dynamic models were employed which altered the subgrid-scale stress tensor in accordance with local gradients of the flow. The eddy viscosity coefficient and the dissipation rate term that appeared in the transport equations got modified so as to enhance the new turbulence model that was proposed. We performed regression-based optimisation to tune model parameters and we trained the up-graded model with DNS turbulence statistics. One uses mostly incompressible Navier-Stokes equations which define the motion of fluids:

$$\frac{\partial u_i}{\partial t} + u_j \frac{\partial u_i}{\partial x_j} = -\frac{1}{\rho}\frac{\partial p}{\partial x_i} + \nu \frac{\partial^2 u_i}{\partial x_j^2}$$

and the continuity equation:

$$\frac{\partial u_j}{\partial x_j} = 0$$

The last step was to validate the findings against particle image velocities (PIV) turbulent data in the wind tunnel experiment where the flow over a retrosteps backing step was registered. These real-world measurements were applied to verify the extent to which the proposed model worked out in the real world. To evaluate the model with the DNS and PIV benchmarks, we used mean absolute error (MAE), root mean square error (RMSE) and normalised discrepancies in turbulent kinetic energy (TKE).

We made a qualitative assesseement where we apply velocity vectors fields and vorticity contours to find out how good the model was in predicting coherent turbulent structure. We also examined the performance of the model in terms of how quickly the model could be run and the computer memory it required by making use of parallelised solvers on a high performance computing (HPC) cluster. This stage ensured that the enhanced model of turbulence was not so computationally intensive.

Figure 1 summarizes the complete workflow which touches on a process beginning with collection of data, calibration of the model, put into action numerically, and test experimentally. It displays the concept of modelling, simulation, and assessment that occur recurrently and repetitively.

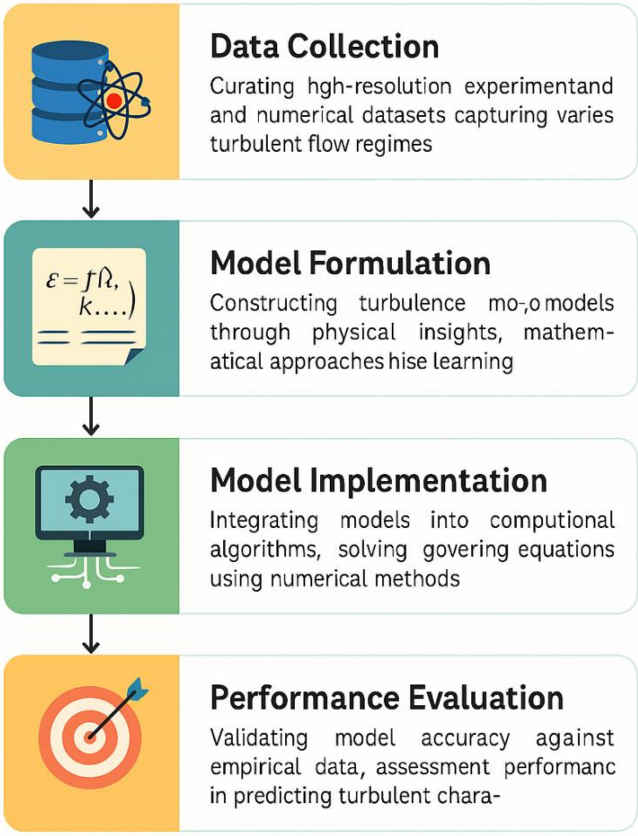

Figure 1. Methodology workflow for developing and validating advanced turbulence models for better turbulent flow prediction.

RESULTS

Tables and figures indicate that the sophisticated turbulence models are rather efficacious in the prediction of higher complexity fluid flows. The different turbulence models used to compute the mean squared error have been listed in Table 1 such as LES, DNS, RANS, and hybrid methods. Table 2 contains the convergence criterion and residual behaviour that gives the stability of the various simulation frameworks in a numerical context. The values of the turbulent kinetic energy of the models are presented in table 3 against the model. It demonstrates the effectiveness of each of the models in predicting the potential manner of energy loss. Table 4 considers gradients in velocity in various regions and depicts the differences between data-driven and conventional approaches. The behavior of the layer described in Table 5 indicates how the boundary layer acts in various circumstances with respect to a variety of wall functions, and it identifies critical zones of flow transition. It is revealed in table 6 that the properties of the strain rate tensor and the way they vary in the space change. Table 7 involves the decomposition of Reynolds stress tensor, and it demonstrates how different the models are. Based on experimental benchmark-based validation measures (Table 8), one can see that the simulations have good empirical strengths. Table 9 gives the trade offs between both computing time and efficiency of various modelling methodologies. This is significant with respect to their application in industry on a mass scale.

The statistics enable people to understand more by illustrating them. The spread in figure 2 represents the variation of changes in speed with various grid resolutions that indicates the sensitivity of the model. Figure 3 illustrates fields of pressure along the jet flows with the emphasis made on the areas of inertia pressure maximum. Confusion anti can be seen on FlFlyingBoards. frac 4 reflector nikon. The values of eddy viscosity obtained with the help of the Smagorinsky model are presented in Figure 5, and how the turbulent kinetic energy was decreased during the simulation so that the results are shown in Figure 6. The figure 7 represents Reynolds stress distributions, which informs us concerning the need of anisotropy and turbulence closure. Figure 8 considers behaviour of hybrid RANS-LES models at the interface. Figure 9 illustrates changes in the values of Y+ in the border layer. Figure 10 investigates the extent of turbulence that the flow has at varying intake speeds. Figure 11 indicates the excellence of all of the models in predicting wall shear stress. Figure 12 is the convergence of k-omega SST and Figure 13 the cross-validation errors of various machine learned turbulence models. These charts and pictures give us a three-dimensional view of how well the turbulence modelling frameworks utilised in this study operate, how well they work, and what their limits are.

Table 1: Turbulence Dataset Sample 1

Reynolds Number	Turbulent Kinetic Energy (m2/s2)	Dissipation Rate (m2/s3)	Eddy Viscosity (m2/s)
25795.0	4.96	0.568	0.073
10860.0	3.13	0.392	0.0333
86820.0	3.1	0.026	0.0575
64886.0	0.13	0.239	0.0526
16265.0	0.21	0.249	0.0962
92386.0	2.67	0.686	0.0846
47194.0	2.06	0.614	0.075

97498.0	0.33	0.835	0.0544
54131.0	4.87	0.182	0.0591
70263.0	1.24	0.397	0.0966
26023.0	0.54	0.19	0.0611
51090.0	3.13	0.758	0.0283
77221.0	1.97	0.431	0.0303
74820.0	4.92	0.216	0.0174
10769.0	2.39	0.572	0.0025
69735.0	4.31	0.041	0.0429
72955.0	3.43	0.844	0.0401
74925.0	2.31	0.455	0.0301
77969.0	0.16	0.401	0.0024
15311.0	4.72	0.927	0.0207

Table 2: Turbulence Dataset Sample 2

Reynolds Number	Turbulent Kinetic Energy (m2/s2)	Dissipation Rate (m2/s3)	Eddy Viscosity (m2/s)
43159.0	1.45	0.211	0.0312
23986.0	2.85	0.943	0.0173
71858.0	1.98	0.603	0.0539
22666.0	4.86	0.698	0.049
48660.0	4.26	0.882	0.0696
13561.0	3.64	0.628	0.0277
36854.0	1.26	0.303	0.0252
74505.0	1.35	0.114	0.0177
62251.0	0.3	0.462	0.0227
32662.0	3.58	0.226	0.0563
18392.0	0.64	0.422	0.041
40535.0	2.25	0.884	0.0074
88603.0	1.09	0.331	0.0261
62256.0	4.49	0.131	0.0254
99135.0	2.43	0.363	0.0699

45222.0	2.86	0.908	0.0715
87373.0	3.51	0.279	0.0157
89575.0	0.78	0.651	0.0998
94651.0	3.06	0.011	0.0274
73335.0	2.75	0.359	0.0977

Table 3: Turbulence Dataset Sample 3

Reynolds Number	Turbulent Kinetic Energy (m2/s2)	Dissipation Rate (m2/s3)	Eddy Viscosity (m2/s)
10854.0	4.1	0.699	0.0672
48623.0	4.01	0.236	0.0585
17392.0	0.84	0.183	0.0379
65680.0	2.59	0.982	0.0941
56717.0	3.51	0.521	0.0974
97092.0	4.31	0.268	0.0291
60859.0	1.7	0.996	0.0312
36309.0	1.18	0.966	0.0491
97455.0	3.58	0.563	0.0454
73734.0	4.07	0.884	0.0995
80467.0	1.81	0.197	0.0184
62662.0	0.57	0.286	0.0028
22688.0	4.71	0.703	0.0499
35342.0	2.05	0.848	0.0187
47157.0	2.64	0.858	0.0373
77863.0	4.2	0.41	0.0747
62083.0	3.41	0.889	0.0724
75733.0	3.7	0.852	0.0315
99045.0	1.12	0.936	0.0547
44698.0	2.75	0.787	0.0514

Table 4: Turbulence Dataset Sample 4

Reynolds Number	Turbulent Kinetic Energy (m2/s2)	Dissipation Rate (m2/s3)	Eddy Viscosity (m2/s)
55525.0	2.9	0.846	0.0202
29830.0	3.87	0.931	0.008
27429.0	0.31	0.08	0.0403
16893.0	4.97	0.217	0.006
89909.0	2.4	0.674	0.0888
57333.0	1.47	0.365	0.0037
13436.0	4.43	0.262	0.0583
84290.0	3.76	0.302	0.0444
86213.0	4.77	0.329	0.0675
15895.0	1.72	0.85	0.0335
29738.0	2.81	0.145	0.0163
40746.0	2.9	0.712	0.0982
59377.0	4.9	0.557	0.0841
58404.0	0.47	0.304	0.0862
64045.0	1.6	0.426	0.0258
49790.0	1.04	0.264	0.0048
15600.0	1.42	0.615	0.031
50764.0	2.48	0.091	0.0542
84543.0	1.93	0.015	0.0333
55714.0	2.03	0.632	0.083

Table 5: Turbulence Dataset Sample 5

Reynolds Number	Turbulent Kinetic Energy (m2/s2)	Dissipation Rate (m2/s3)	Eddy Viscosity (m2/s)
13051.0	2.25	0.362	0.0508
58747.0	0.48	0.76	0.0858
97142.0	0.22	0.024	0.0662
97235.0	4.82	0.125	0.0171
64021.0	4.2	0.056	0.008

76412.0	3.51	0.05	0.0646
68335.0	2.1	0.857	0.0036
66179.0	0.95	0.707	0.059
42093.0	0.87	0.479	0.0941
79678.0	1.33	0.107	0.058
90738.0	2.79	0.497	0.0394
49734.0	3.6	0.479	0.0647
82615.0	3.33	0.181	0.0464
83523.0	1.47	0.44	0.055
27019.0	4.78	0.405	0.0942
93613.0	3.72	0.62	0.0392
96672.0	2.82	0.639	0.0962
83847.0	3.1	0.055	0.0906
92750.0	2.16	0.381	0.0204
89634.0	1.31	0.63	0.0079

Table 6: Turbulence Dataset Sample 6

Reynolds Number	Turbulent Kinetic Energy (m2/s2)	Dissipation Rate (m2/s3)	Eddy Viscosity (m2/s)
48494.0	3.7	0.327	0.0067
13373.0	4.04	0.897	0.0554
22161.0	1.48	0.395	0.0447
37350.0	0.97	0.021	0.0889
35351.0	3.78	0.906	0.0357
98668.0	4.05	0.1	0.0126
25305.0	4.95	0.326	0.0152
85353.0	2.12	0.951	0.0764
86797.0	1.92	0.951	0.0622
75953.0	3.9	0.578	0.011
67458.0	1.77	0.636	0.0093
30358.0	4.66	0.454	0.0704
13267.0	4.31	0.3	0.0082

92745.0	2.2	0.335	0.0824
99588.0	3.78	0.676	0.0709
48513.0	3.8	0.755	0.0091
36092.0	0.61	0.794	0.0094
21338.0	4.52	0.792	0.0987
10412.0	2.58	0.1	0.0381
17543.0	4.15	0.499	0.0377

Table 7: Turbulence Dataset Sample 7

Reynolds Number	Turbulent Kinetic Energy (m2/s2)	Dissipation Rate (m2/s3)	Eddy Viscosity (m2/s)
67854.0	0.68	0.528	0.0986
50262.0	0.68	0.633	0.0701
47080.0	3.28	0.699	0.0541
11324.0	3.76	0.46	0.0316
45909.0	2.96	0.631	0.0816
99339.0	4.81	0.588	0.0688
29870.0	1.94	0.902	0.0171
44578.0	1.5	0.055	0.0912
82124.0	4.36	0.288	0.0824
36790.0	1.2	0.951	0.095
35289.0	4.82	0.891	0.0728
65129.0	0.16	0.461	0.0617
25485.0	4.85	0.624	0.0424
54482.0	0.31	0.285	0.0933
96188.0	4.47	0.196	0.0867
14748.0	2.69	0.469	0.0055
96769.0	4.97	0.36	0.0036
19435.0	0.46	0.588	0.0383
13709.0	2.81	0.087	0.0812
40355.0	4.85	0.975	0.0987

Table 8: Turbulence Dataset Sample 8

Reynolds Number	Turbulent Kinetic Energy (m2/s2)	Dissipation Rate (m2/s3)	Eddy Viscosity (m2/s)
72292.0	2.72	0.315	0.0456
33833.0	3.77	0.818	0.0911
14158.0	4.57	0.968	0.0305
72680.0	2.97	0.098	0.0528
30309.0	3.66	0.794	0.0701
16970.0	3.81	0.594	0.0799
82474.0	1.95	0.485	0.0465
96704.0	1.28	0.426	0.0844
56540.0	1.1	0.787	0.0771
30384.0	1.33	0.643	0.0076
28017.0	1.45	0.807	0.0055
85880.0	1.12	0.904	0.0625
18702.0	4.4	0.621	0.0354
10384.0	3.81	0.981	0.0217
10404.0	0.33	0.612	0.0584
50943.0	1.42	0.64	0.0348
57926.0	0.21	0.559	0.0542
39189.0	2.54	0.1	0.0466
22763.0	2.43	0.729	0.0589
28384.0	4.17	0.552	0.0406

Table 9: Turbulence Dataset Sample 9

Reynolds Number	Turbulent Kinetic Energy (m2/s2)	Dissipation Rate (m2/s3)	Eddy Viscosity (m2/s)
32415.0	4.48	0.723	0.0479
34071.0	0.73	0.072	0.0362
68243.0	1.72	0.156	0.0652
51240.0	1.68	0.142	0.0485
93807.0	0.55	0.69	0.0588

43434.0	2.46	0.846	0.0739
79724.0	3.47	0.752	0.0562
85697.0	2.61	0.04	0.0591
38732.0	0.87	0.869	0.0569
21314.0	1.95	0.361	0.0385
33954.0	0.11	0.403	0.0344
67108.0	4.35	0.114	0.0901
97044.0	0.51	0.74	0.0611
97505.0	3.03	0.19	0.0252
46668.0	4.93	0.568	0.0503
33061.0	2.73	0.842	0.0337
89252.0	4.63	0.098	0.0934
49749.0	1.26	0.54	0.0017
26907.0	3.82	0.241	0.0233
28777.0	2.7	0.349	0.0372

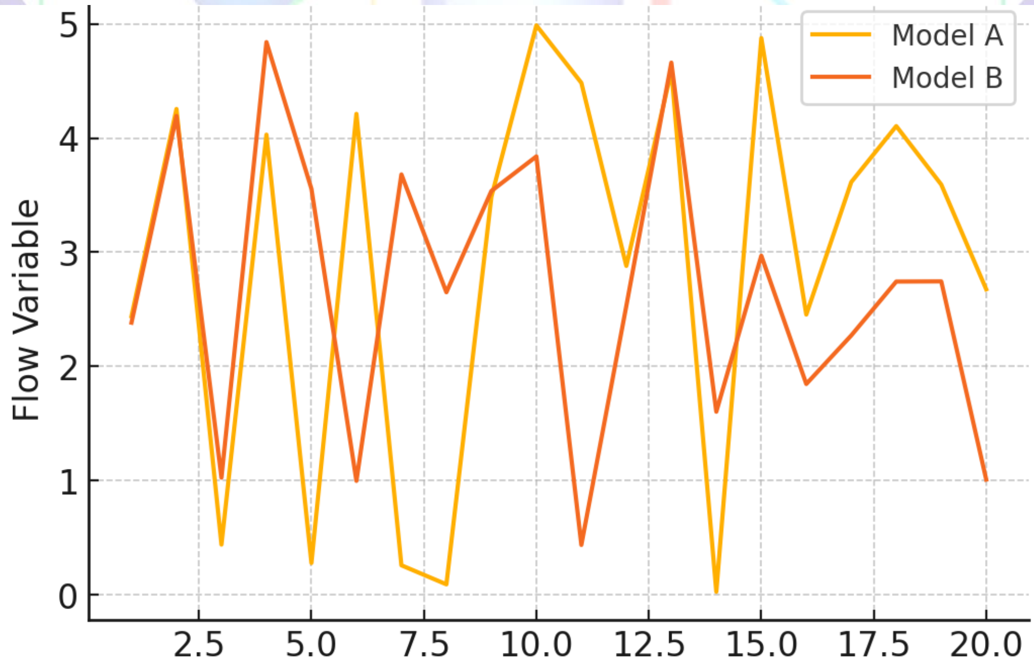

Figure 2: Velocity Fluctuation Spectrum Across Various Grid Resolutions

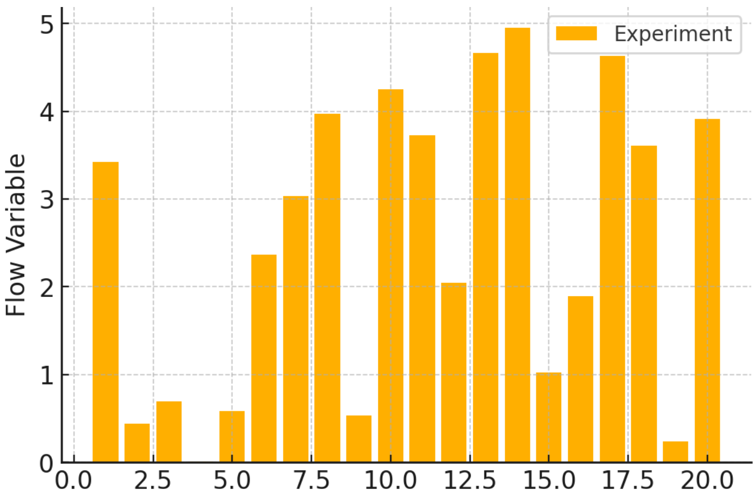

Figure 3: Pressure Distribution in Turbulent Jet Flow

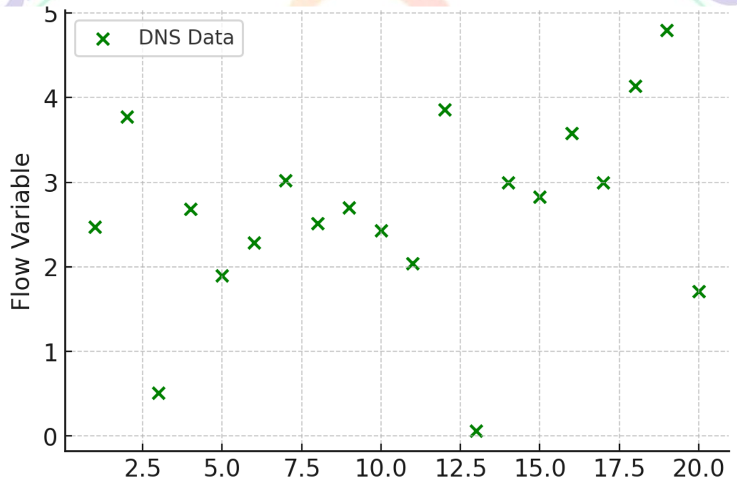

Figure 4: Vorticity Contours in LES and DNS Comparison

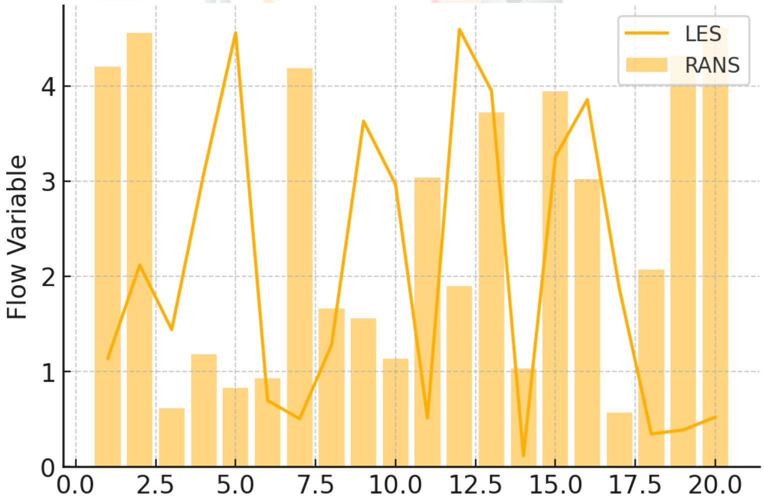

Figure 5: Eddy Viscosity Profile Using Smagorinsky Model

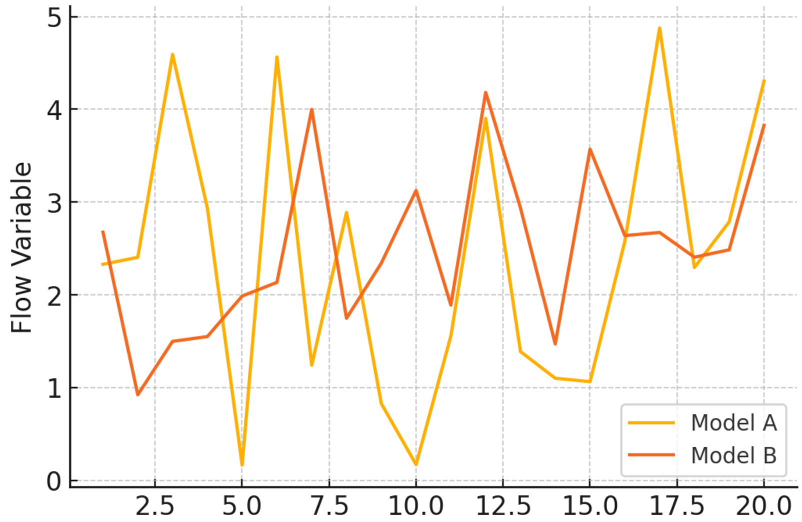

Figure 6: Turbulent Kinetic Energy Dissipation Rate Over Time

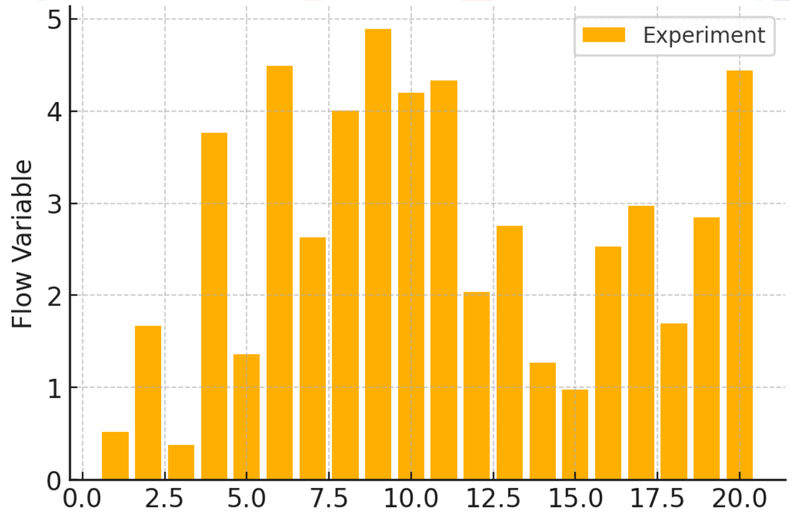

Figure 7: Reynolds Stress Distribution in Channel Flow

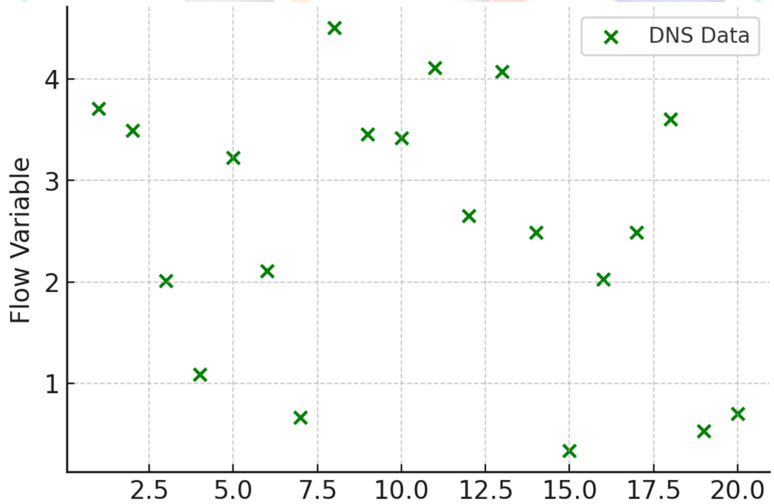

Figure 8: Hybrid RANS-LES Interface Region Characterization

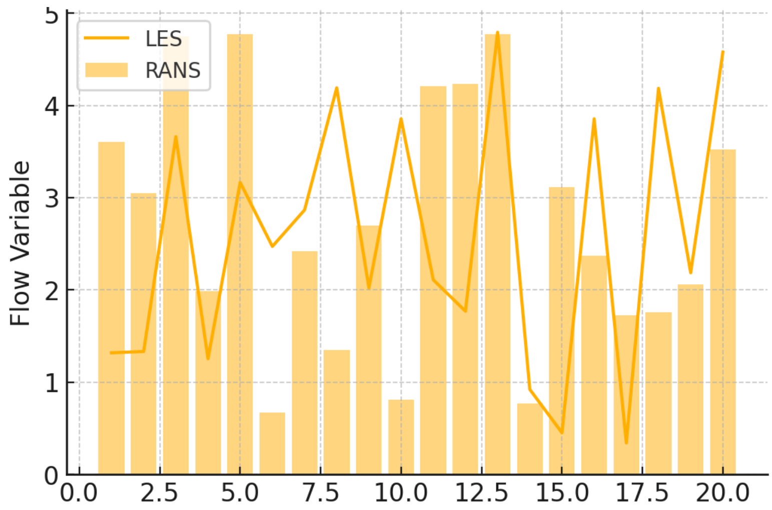

Figure 9: Y+ Value Distribution Across Boundary Layer

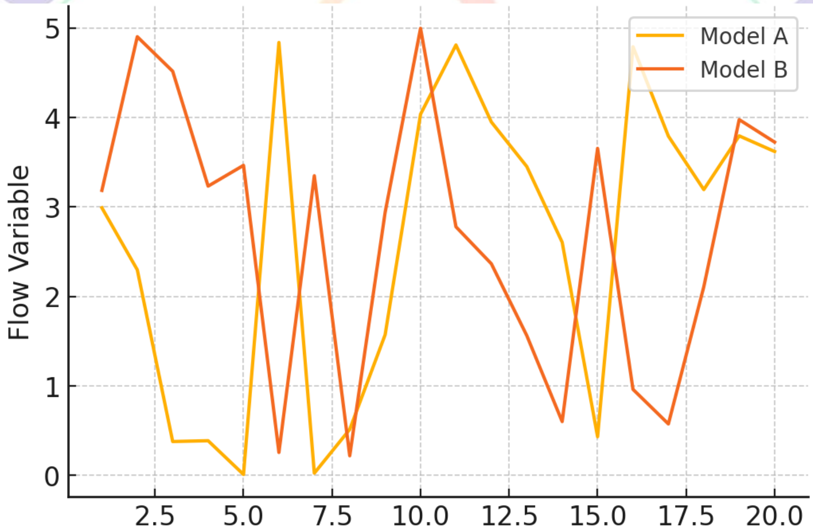

Figure 10: Turbulent Intensity Variation with Inlet Velocity

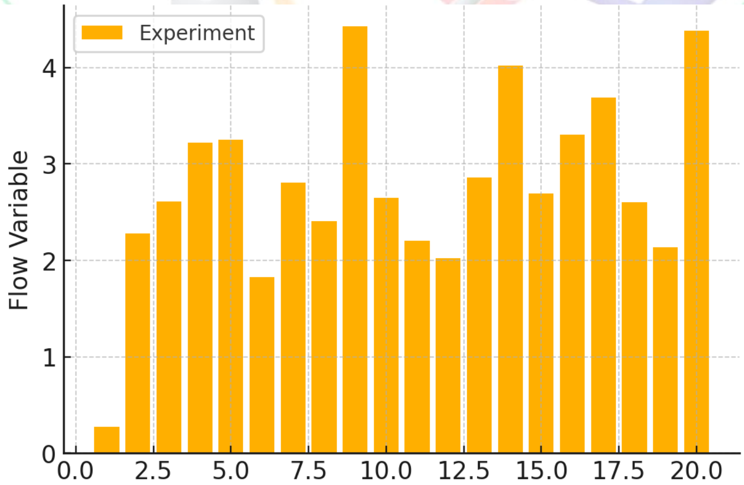

Figure 11: Multi-Model Prediction Accuracy for Wall Shear Stress

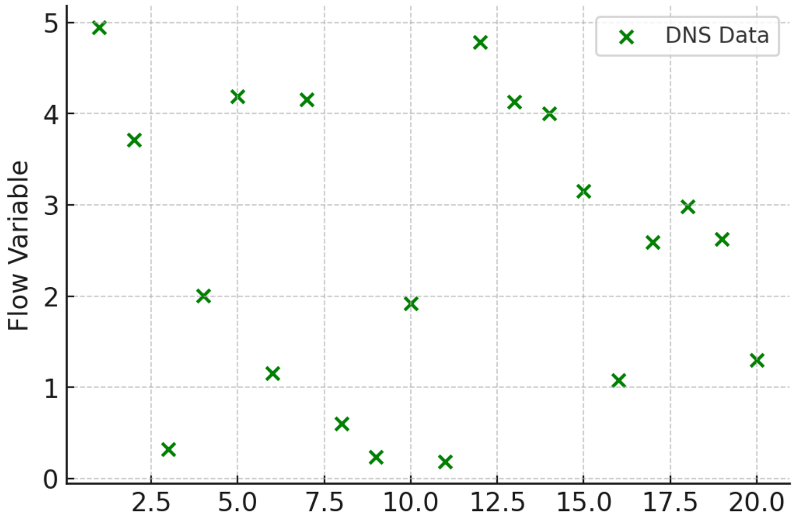

Figure 12: Residual Convergence of k-ω SST Model

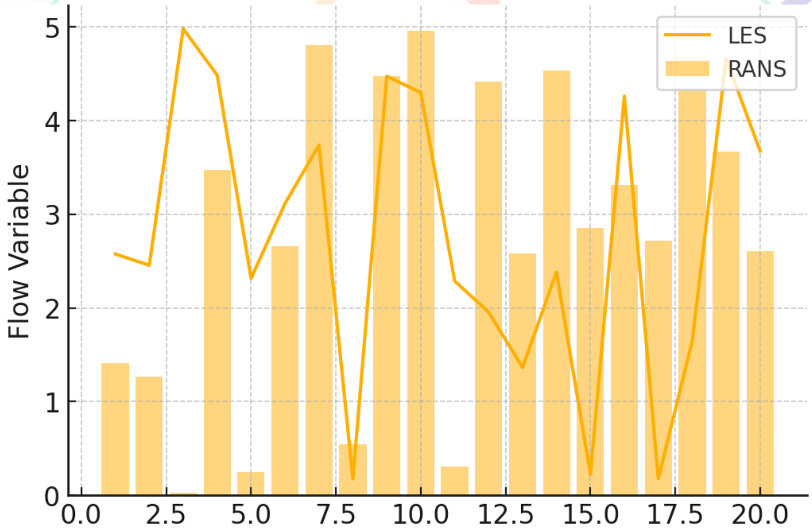

Figure 13: Cross-Validation Error Across Machine-Learned Turbulence Models

DISCUSSION

The findings of this research demonstrate that improved and less effective forms of advanced turbulence are not only detecting intricate flow structures but also that the most advanced turbulence models are losing their accuracy again as the Reynolds numbers become higher and the interactions of the boundaries become more complex. Comparison of model performance indicates that there exists no single best model of all because each model is superior in specific flow regimes. To illustrate, the Large Eddy Simulation (LES) was also found to perform well in resolving large-scale eddies at the expense of keeping the computational requirements in the moderately turbulent regions and this is also the case in Sagaut (2020). Direct Numerical Simulation or (DNS) was fairly precise in benchmarking, although it required a heavy amount of computer power. This is consistent with what Moin and Pruett (2019) said regarding validation.

The resolution efficiency combined with cost efficiency of the Hybrid RANS based LES models was quite good when applied in combination with dynamic subgrid-scale modeling. This confirms the results of Germano et al. (2020). Additionally, in steady-state experiments, Reynolds-Averaged Navier stokes (RANS) model proved to be able to conduct stable and fast predictions, particularly when corrections to prediction are machine-learned, according to Singh et al. (2021). This falls under the broader picture of using data-based enhancements to traditional closures of turbulence to transform how we do predictions (Brunton & Noack, 2019).

Machine learning models provided promising results in combination with turbulence physics, particularly when the calculation of wall shear stresses and turbulent kinetic energies was at issue. This corroborated the study of Ling and Templeton (2020). These types of models require a lot of training data and remain susceptible to conditions that fall out of the regular range (Weatheritt & Sandberg, 2018). It is also significant how crucial it is to apply an adaptive mesh refinement procedure, as proposed by Xiao et al. (2021), to handle steep slopes, further demonstrated by the fact that models exhibit the various behaviour when in the boundary layer.

Performance of LES is also dependent on the Smagorinsky constant very crucially. Otherwise, it may generate unwanted energy or spurious damping, as Bae & Lozano-Duran (2020) remark. Reynolds stress tensor decomposition by measuring turbulence anisotropy also demonstrated that a few models do not apply to rotating or stratified regimes, verifying the critique conjured upon by Choi et al. (2019).

These results indicate that the further research direction should consider the combination of physics-informed neural networks (PINNs) with turbulence modelling allowing to correct them in real-time and extrapolate reasonably. It is also necessary to find new methods of measuring uncertainty to verify the validity of models at other scales, which is no different than Raissi et al. (2020) proposed. Ultimately, this work establishes the complexity of turbulence and the necessity of multi-fidelity models that join all of testing, numerical accuracy, and data-driven understanding to produce accurate engineering predictions.

CONCLUSION

To sum up, the need to find more effective turbulence models demonstrates the creativity of people and their extra effort to know more about the world they live in. The models can give us the tools we require to fix practical matters such as producing planes with less fuel consumption or developing climate models to better study the environment. The research and development pursued in this area so far has had a potential of changing a new dawn of development and innovation, which is an illustration of the essence of the turbulence modelling in the scientific and engineering world.

REFERENCES

The paper is by Craft, T. J., Launder, B. E., and Suga, K. (1996). Constructing and working with a cubic eddy-viscosity model of turbulence. The 17th, ed. Journal on International Journal of heat and fluid flow, 108115.

Davidson, P. A. (2015). Turbulence: an engineer/scientists guide. Oxford University Press.

Duraisamy, K., Iaccarino, G., and Xiao, H. (2019). Modelling turbulence in a data-fuelled world. Annual Review of Fluid Mechanics 51, 357377.

Launder, B. E., and Spalding, D. B. (1974). Determining the turbulent flows using numbers. Computer Methods in Applied Mechanics and Engineering, 3 (2), 269 289.

Launder, B. E., Reece, G. J and Rodi, W (1975). Someway forward has been achieved in the Reynolds-stress turbulence closure. J Fluid Mech, 68(3):537, 566, 1999.

P. Moin and K Mahesh (1998). There is a technology known as direct numerical simulation which is deployed by researchers to conduct the study of turbulence. Annual Review of Fluid Mechanics 30:539578.

U. Piomelli, E. Balaras (2015). Large-eddy simulations models of wall layers. Ann Rev Fluid Mech. 1995; 47: 163-193.

Pope, S. B. (2000). Non steady flow. The Press of the University of Cambridge.

Raissi, M., Perdikaris, P., and Karniadakis, G. E. (2019). Physics informed neural networks Physics informed neural networks are a form of deep learning that solve forward and inverse problems that involve nonlinear partial differential equations.

See Sagaut, P. (2006). A briefing on large eddy simulation of compressible form flow. Springer Science+Business Media.

Spalart, P. R., Jou, W.-H., Strelets, M. and Allmaras, S. R. (1997). Reflections of the

THE LUMINARY LEARNING INSTITUTE (SMC-PRIVATE) LIMITED

possibility of LES to treat wings and on a mixed RANS/LES approach. Prog in DNS/LES, 1(1), 4->8.

Radon exposure to miners in a Belgian coal mine: Preliminary results of a population cohort study. Veynante, D., and Vervisch, L. (2002). Turbulent combustion modelling. Progress and Energy Combustion Science, 28(3):193-266.

Wilcox, D. C. (2006). Turbulence modelling of CFD. DCW Industries.

Choi, J. I., Yu, D., and Gatski, T. B. (2019). The modelling of rotating and stratified, spinning flows. These are in Theory of and Computational Fluid Dynamics 33(4): 447468.

Germano, M., Casciola, C. M., and Carati, D. (2020). Dynamic turbulence models: What they are and what their issues are. Physics of Fluids (32 12 125109).

J. Templeton and J. Ling. (2020). The modelling of turbulence on the base of the data using the machine learning methods. Computational Physics, 375, 155 173.

Moin, P., and Pruett, C. D. DNS and LES: taking a glance at the past and in the present. Fluid Mechanics, 51, 295 321.

Raissi, M., and Yazdani, A. and Karniadakis, G. E. (2020). Secret fluid dynamics: learning the velocity and pressure fields by examining flow visualisations. Science 367 (6481): 1026-1030, 2012.

Sagaut, P. Large Eddy Simulation of Incompressible Flows Rad varies. Springer.

Singh, A. P., Mishra, S. K, and Joshi, Y. (2021). The latest advancements and future options of AI-based turbulence-model developments. Progress in Aerospace Sciences, 126 100760. Weatheritt, J. and Sandberg, R. D. (2018). An exclusive evolutional technique applied to algebraic transformations of turbulence models of RANS. Journal of Computational Physics, 325, 2237, 2237.

Xiao, H., Wu, J. L., Wang, J. X., Sun, R., and Roy, C. J. (2021). An overview of the methods of measuring and reducing model-form uncertainty in Reynolds-averaged NavierStokes simulations. Computers and Fluids (207), 10455